Characterization of GOCE SSTI Antennas

Florian Dilßner, Günter Seeber, Martin Schmitz, Gerhard Wübbena,
Giovanni Toso and Damien Maeusli

Summary
Within the framework of the European GOCE mission, which is scheduled for launch in 2007 by the European Space Agency (ESA), a high accuracy Satellite-to-Satellite Tracking Instrument (SSTI) with two hemispherical-coverage receiving antennas will be used for real time navigation and precise orbit determination. The two GPS antennas are directly mounted on the edge of one of the metallic solar array wings of the spacecraft. Besides of antenna phase center variations (PCV), near field effects like multipath, diffraction and imaging induced by the close vicinity of the antenna can seriously affect the measurement performance of the SSTI. Therefore, several experiments with engineering models of the GPS antennas were performed using the Automated Absolute Field Calibration Technique developed by the Institut für Erdmessung (IfE) of the University of Hannover and Geo++ at Garbsen (Germany). In order to characterize the interactions with the spacecraft, the GPS antennas were first calibrated in standalone mode and finally also together with a representative cut-out of GOCE's solar wing which was mounted beneath the antennas. The differences of both set-ups in terms of PCV as well as carrier to noise ratio (C/No) reveal the influence of the near field effects caused by the wing. Extensive electromagnetic simulations done at ESA's European Space Research and Technology Centre (ESTEC) have confirmed the results. First tests on the final antenna flight-models show performance improvement.

Zusammenfassung
Im Rahmen der Europäischen GOCE-Mission, deren Weltraumstart unter Leitung der European Space Agency (ESA) voraussichtlich im Jahr 2007 erfolgen soll, wird ein hochgenaues Satellite-to-Satellite Tracking Instrument (SSTI) mit zwei Empfangsantennen zur Echtzeitnavigation und präzisen Bahnbestimmung eingesetzt. Die beiden GPS-Antennen sind unmittelbar auf der metallischen Oberfläche eines der Solarzellenflügel des Satelliten angebracht. Somit sind neben Variationen des Antennenphasenzentrums (PCV) auch zusätzliche Nahfeldeinflüsse wie Mehrwegeeffekte, Diffraktion und Imaging zu erwarten, die die Datenqualität des SSTI erheblich verschlechtern können. Aus diesem Anlass wurden diverse Untersuchungen mit Hilfe des am Institut für Erdmessung der Universität Hannover und bei der Garbsener Firma Geo++ entwickelten Verfahrens der Automatisierten Absoluten Feldkalibrierung an »Engineering Modellen« der GPS-Antennen durchgeführt. Um die Auswirkungen der Nahfeldeffekte abschätzen zu können, wurden die GPS-Antennen zunächst für sich allein und anschließend zusammen mit einem repräsentativen Modell eines Flügels des GOCE Satelliten kalibriert, der an der Antennenunterseite montiert wurde. Die Differenzen aus beiden PCV-Datensätzen sowie aus den Signal/Rausch-Verhältnissen (C/No) zeigen den Einfluss der Nahfeldeffekte auf, die durch den Flügel hervorgerufen werden. Umfangreiche elektromagnetische Simulationen am European Space Research and Technology Centre (ESTEC) bestätigen die Ergebnisse. Erste Tests mit den endgültigen Flugmodellen der Antennen zeigen weitere Verbesserungen.

1 Introduction

The Gravity Field and Steady-State Ocean Circulation Explorer (GOCE) is dedicated to measure the Earth's gravity field for modelling the geoid on a global scale with high spatial resolution and accuracy. As part of ESA's Living Planet Programme, it is the first Earth Explorer Core mission and is scheduled for launch in 2007 from Plesetsk Cosmodrome in Northern Russia. The satellite will be positioned in circular, near-polar, sun-synchronous orbit with a mean orbital altitude of 250 km.

Besides of a state-of-the-art Electrostatic Gravity Gradiometer as the primary measurement unit for providing the short wavelength terms of the geopotential, the pay-

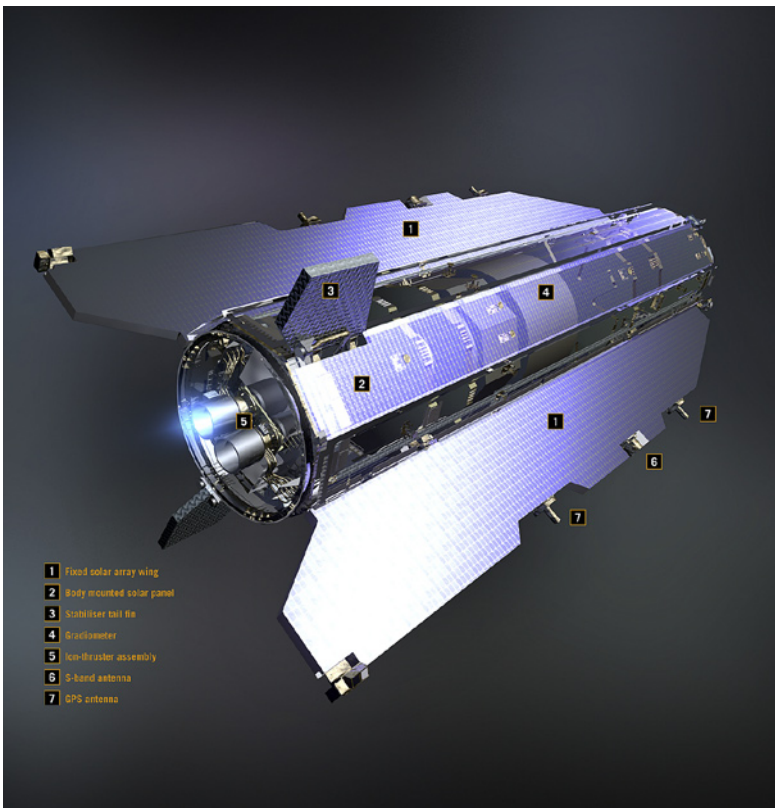

Fig. 1: GOCE spacecraft with payload (provided by ESA)

load of GOCE includes a Satellite-to-Satellite Tracking Instrument (SSTI) which consists of two advanced dual-frequency, 12-channel LAGRANGE GPS receivers and two hemispherical-coverage L-band antennas for multi-high-low tracking between the satellites of the GPS constellation and the low flying GOCE spacecraft (Fig. 1). The two receiver/antenna pairs will be operated in cold redundancy. The goal of the SSTI is to obtain pseudo-range and carrier-phase data with a sampling rate of 1 Hz for real time navigation as well as for precise orbit determination (POD) allowing a high accurate retrieval of the long wavelength terms of the gravity field. The POD task will be validated by Satellite-Laser-Ranging observations.

The GOCE orbit products will be generated with a reduced-dynamic and a purely kinematic POD approach. In order to ensure a reliable positioning accuracy of about 1 cm for the precise orbit computations, the electrical phase variations of the GPS antennas have to be determined by a suitable calibration technique. The GOCE SSTI requirements on that calibration procedure are quite high. According to an elevation cut-off angle of 15°, the maximum error on the phase center position should not exceed 1.8 mm for the L1 and 2.4 mm for the L2 carrier phase signal. The challenge is further increasing when so-called near field effects like multipath, diffraction and imaging induced by the presence of the GOCE spacecraft modify the antenna phase variations. The maximum phase error caused by such near field influences shall be lower than 3.2 mm for L1 and 4 mm for L2.

For the characterization of the antenna phase variations with the required accuracy, besides other actions initiated by ESA, the Automated Absolute Field Calibration Technique developed by the Institut für Erdmessung (IfE) and Geo++ has been used (Wübbena et al. 2000). Due to rapid changes of the antenna orientation through a moving robot, absolute phase center offsets and variations (PCV) are determined on submillimeter level while unwanted multipath interferences caused by reflecting surfaces of the site environment (roofs, walls, etc.) are completely eliminated. Additionally, as an indicator for the GPS antenna gain behaviour, a hemispherical pattern of the carrier to noise ratio (C/No) is evaluated in order to verify e. g. the symmetry of gain in different azimuth directions. Furthermore, the influence of the GOCE solar panel on phase and amplitude is estimated by calibrating the GPS antennas not only in stand-alone mode but also together with a representative cut-out of the spacecraft's solar wing which was mounted beneath one single GPS antenna. The differences of both set-ups confirm and identify the near field influences caused by the wing. The magnitude of the detected effects on the PCV as well as their impact in the positioning domain underline that such errors must be taken into account in order to fully meet the accuracy requirements of the GOCE SSTI application. Within this contribution, we report on tests and first results obtained with the Automated Absolute Field Calibration Technique.

2 Background

2.1 Antenna Phase Variations

It is well known that any kind of GPS measurement refers to the electrical phase center of the antenna, which is neither a physical nor a stable point. Actually, the measured phase depends on the azimuth a and elevation angle e of the particular satellite position (Fig. 2). Moreover, the location varies with the intensity and the carrier frequency of the incident signals.

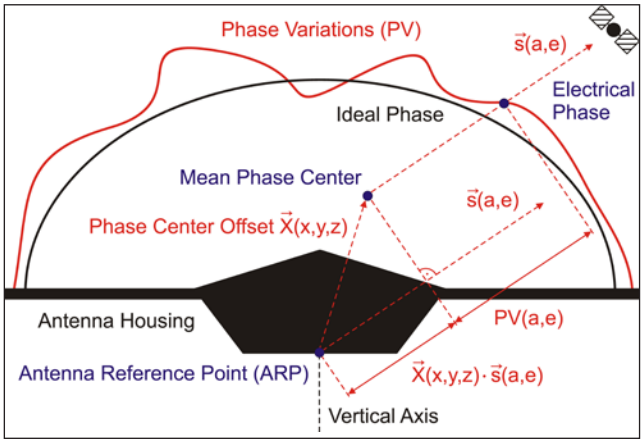

Fig. 2: Relationship between the external antenna reference point, mean phase center and antenna phase variations

In order to refer GPS measurements to a well defined geometrical point, the vector between the actual phase measurement and an external antenna reference point (ARP) on the antenna has to be known. For most antenna types, this ARP is defined as the intersection of the vertical axis with the lowest part of the antenna housing. The spatial coordinates of a mean electrical phase center for the particular carrier signal with respect to this ARP are representing the so-called phase center offset $\vec{X}$, which is often given by the manufacturers as a rough and approximate correction. The location of the mean phase center can be interpreted as the center of a spherical surface (with fixed but arbitrary radius) approximating the real phase front. The deviations of the actual electrical phase from the mean phase center are denoted as phase variations (PV). Referring to this, the commonly used term »Phase Center Variations (PCV)« is slightly misleading, because it suggests a varying center with spherical wave fronts. The overall correction between the antenna's external reference point and its electrical phase center is given by

$$PV_{ARP}(a,e) = \vec{X}(x,y,z)\cdot\vec{s}(a,e) + PV(a,e) \qquad (1)$$

where $\vec{s}$ represents the normalized antenna-satellite vector. Thus it appears that a mean phase center offset is not essentially required as the effect can be described exclusively by the elevation- and azimuth dependent phase variations.

Antenna phase variations can reach magnitudes in the order of several millimeters up to a few centimeters. Using linear combinations of L1 and L2 like the ionospheric-free signal L0, the bias will be amplified by a factor of about 3. This aspect is of particular relevance for Satellite-to-Satellite-Tracking (SST) applications, because mostly a mean orbital altitude is chosen where ionospheric propagation delays still play a non-negligible role.

In ground-based geodetic applications neglecting the phase center variations is rather critical because of correlations between PCV and tropospheric errors. In particular for precise height determination within larger networks, the knowledge of PCV plays a very important role, because missing information about PCV will be misinterpreted as tropospheric refraction and therefore falsifies the height component. In space-based applications like SST this aspect may be of minor importance.

Because antennas of the same type and model usually show similar PCV, their effects can already be reduced in relative positioning within smaller networks by orienting the antennas to the same direction. For highest accuracy requirements, in any case it is necessary to calibrate the antennas. In order to be able to describe the antenna phase variations, several calibration procedures have been developed during the last years. The first group is formed by relative field calibrations on short-baselines estimating phase center offsets and variations with respect to a given reference antenna (Mader 1999). The methods are based upon the assumption that the PCV of the reference antenna are equal to zero or are taken as known. The observations are distributed heterogeneously and contain site-dependent multipath effects. Therefore, it is difficult to determine azimuthal PCV and the elevation angle is generally limited to 10°. The results cannot be applied in case of differently orientated antennas (e. g. rotated or inclined antennas as well as on long baselines). The second group is formed by absolute antenna calibration techniques. Besides of measurements using artificial GPS signals in anechoic chambers (Schupler et al. 1994, Görres et al. 2004), the Automated Absolute Field Calibration based on a high-precision robot-system is in operational use (Wübbena et al. 2000).

2.2 Carrier To Noise Ratio

The carrier to noise ratio (C/No) can be considered as another key parameter describing the measurement performance of a GPS system, because it determines how well the receiver's code- and carrier-tracking loop can process the signals and therefore how precisely pseudoranges and carrier phases can be obtained (Langley 1997). It is a measure of the received carrier signal strength relative to the strength of the received noise and is commonly expressed in decibel-hertz (dB-Hz). The larger the C/No value, the stronger the signal. The level finally measured at the receiver's correlator input is a sum of several gain and loss parameters of the transmission line between satellite and receiver (e. g. satellite transmitting power, antenna gain, cable loss, receiver noise). Moreover, the carrier to noise ratio can be amplified or attenuated due to the superposition of additional multipath signals.

2.3 Automated Absolute Field Calibration

During the last years, the Automated Absolute Field Calibration has proven to be one of the most accurate techniques for the determination of absolute antenna phase center offsets and variations. The fundamental concept of this calibration method is based on the rigorous separation between antenna phase variations and site dependent multipath effects. Other than for relative calibration approaches, the results are completely independent from environmental multipath as well as the phase center characteristics of the used reference antenna. By means of a precisely calibrated and fast moving robot, the test antenna is tilted and rotated (Fig. 3). These quick changing antenna orientations are essential for the calibration. Since time differences between consecutive epochs amount to just a few seconds, the environmental multipath error is highly correlated and can be well described as a stochastic process within a Kalman filter. To avoid any potential multipath not eliminated by mathematical modelling, a high elevation mask of 18° is used, which is dynamically adopted for tilted orientations. Further error components such as ionospheric, tropospheric and orbit biases cancel out using a very close-by reference station. Due to this observation procedure, it is possible to ob-

Fig. 3: Robot with Quadrifilar Helix antenna mounted on GOCE solar wing cut-out during absolute antenna calibration

tain ultimately a clear PCV signal free of residual systematic effects.

Depending on the particular satellite constellation, one calibration data set consists of a dense and homogeneous coverage of around 6000 to 8000 measurement epochs without any geographical station dependencies like the northern hole. The model describes the complete antenna hemisphere down to zero degree elevation by means of a spherical harmonic expansion of degree $n_{\max}$ and order $m_{\max} \leq n_{\max}$. Hence, the resulting phase center variations are elevation as well as azimuth dependent. Measurements below the antenna horizon (–5°) are operationally incorporated to strengthen the model at zero degree elevation. For each carrier frequency and C/No signal, the spherical harmonic coefficients a_{nm} and b_{nm} of the following function are estimated within the Kalman filter process:

$$PV_{ARP}(a,e) = \sum_{n=0}^{n_{\max}} \sum_{m=0}^{m_{\max}} \left(a_{nm} \cos ma + b_{nm} \sin ma\right) \cdot P_{nm}(\sin e). \quad (2)$$

P_{nm} are the standardized Legendre polynomials of first kind. The low coefficients of this function represent the components of the antenna offset vector $\vec{X}$. The PCV value in zenith direction is explicitly set to zero. A corresponding hemispherical pattern of the carrier to noise decrease can be generated in a similar way.

The accuracy and reliability of the Automated Absolute Field Calibration has been extensively analyzed in recent years. Various investigations with different robots, on different stations, at different times have demonstrated the excellent quality of the PCV determination (Menge 2003). Standard deviations in the range of 0.2 to 0.4 mm induce a repeatability of approximately 1 mm. Görres et al. 2004 have shown that absolute calibrations from anechoic chamber measurements and robot agree at the 1 mm level if an individual antenna is calibrated. Due to all these advantages, the International GNSS Service (IGS) meanwhile intends to implement operationally absolute phase corrections based on robot calibrations of among 40 of their station antennas (Gendt and Schmid 2005). The official switch to absolute calibration models within the IGS tracking network will be done in April/May 2006 (Gendt 2005).

2.4 Antenna Near Field Effects

Antenna near field effects are mainly caused by multipath interferences induced by reflectors located in the close vicinity of the antenna as well as other electromagnetic phenomenas like diffraction and antenna imaging effects. Such effects can significantly change phase and amplitude characteristics of a GPS antenna. In ground based geodetic applications, it is known that near field effects are usually caused by surfaces of pillars or special adaptations where the antennas are mounted on (Elosequi et al. 1995, Wübbena et al. 2003). In case of Satellite-to-Satellite-Tracking applications like GOCE, it is the body of the LEO spacecraft which is responsible for this kind of unwanted distortion.

There are different reasons why multipath effects coming from nearby objects can cause more severe problems in precise GPS positioning compared to multipath induced by reflectors which are located further away from the antenna. First, due to the short distance between the reflector and the antenna phase center, the reflected signals tend to be much stronger than signals coming from more distant objects because they experience less spreading loss. Hence, the amplitude of these multipath errors is larger.

Second, the antenna near field multipath has a very long-periodic behaviour, especially with increasing satellite elevation angles. Depending on the height of the antenna above the reflecting horizontal surface, the multipath periods of oscillation can reach several hours (Fig. 4). Therefore, the influence on the positioning results does

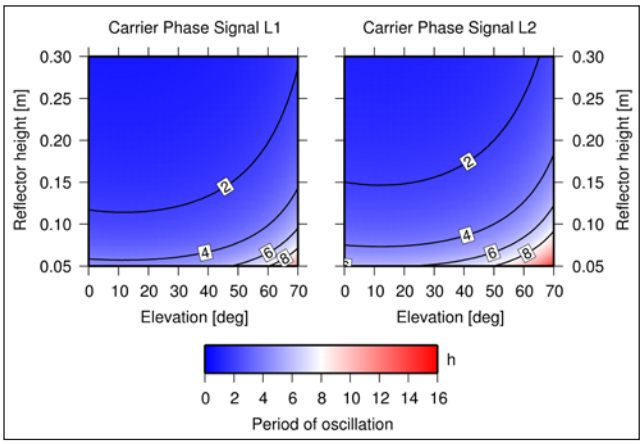

Fig. 4: Typical oscillation periods of several hours of the near field multipath on the carrier signals L1 (left) and L2 (right)

not average out for the near field. Only distant reflector's multipath with high frequency can be reduced effectively by averaging over sufficient periods of time.

Moreover, todays receiver based mitigation techniques against carrier phase multipath are still ineffective in case of short excess signal paths. If the direct signal and the indirect signal arrive just within approximately 100 nanoseconds or 30 meters, the receiver processing algorithms cannot distinguish between the desired direct signal and the reflected signal (Weill 2003).

In order to detect the appearance and to reveal the magnitude of antenna near field effects, the Automated Absolute Field Calibration has proven to be a well suitable technique (Wübbena et al. 2003, Schmitz et al. 2004). For this type of investigation, the antenna has to be mounted on the robot together with a representative model of the real antenna environment. During the calibration process, this near-by surface model will now cause multipath in-

terferences. Because the geometric relationship between antenna and environment cut-out is constant, reflections coming from the same direction with respect to the antenna coordinate system induce the same multipath signal. Therefore, the antenna near field effect is not eliminated by the calibration observation procedure. Instead, an additional signal pattern caused by the near field multipath superimposes the PCV signal. Comparing the measured pattern with the PCV results of the isolated antenna calibration, the influence of the near field can be estimated and analyzed.

3 GOCE SSTI Antennas

The GOCE SSTI antennas are directly installed on top of the solar array wing of the spacecraft (Fig. 5). In order to balance mass, two dummy antennas are mounted on the opposite wing. Due to restricted space in the rocket fairing while, at the same time, trying to maximize available solar array (and power) aboard the satellite, the antennas are installed in a cut-out of the array itself. Looking at the geometrical configuration (Fig. 6), one can expect that the most critical interactions with the spacecraft will be caused by this solar array wing, especially for the antenna located in position A2 of Fig. 5. Numerical simulations at ESA/ESTEC have confirmed this assumption (Polimeni 2004).

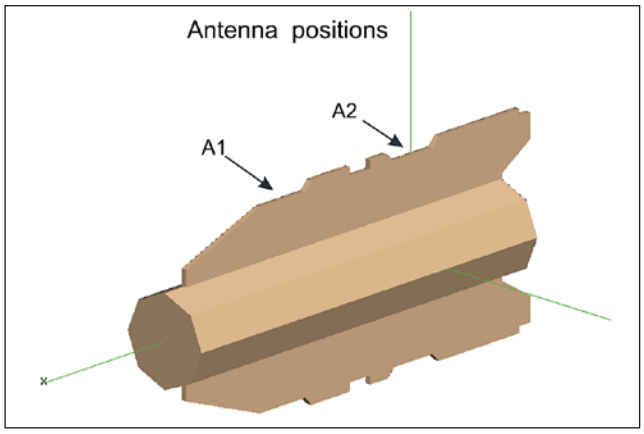

▲ Fig. 5: Positions of SSTI antennas on GOCE solar wing

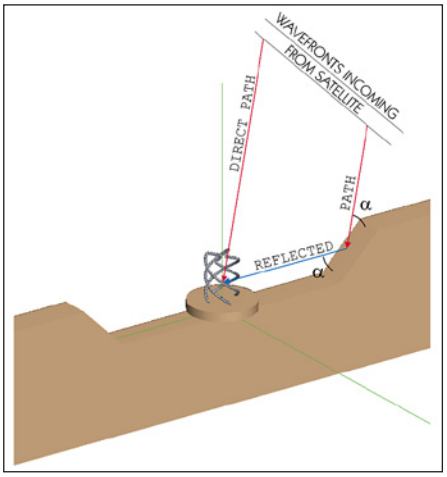

◄ Fig. 6: Multipath effect of GPS signal on GOCE solar wing

Originally two different GPS antenna candidates were considered for setting up the SSTI instrument of the GOCE mission, a helix antenna as the baseline and a patch antenna as a possible back-up candidate (Fig. 7). Both have dual-frequency capability and are so-called passive

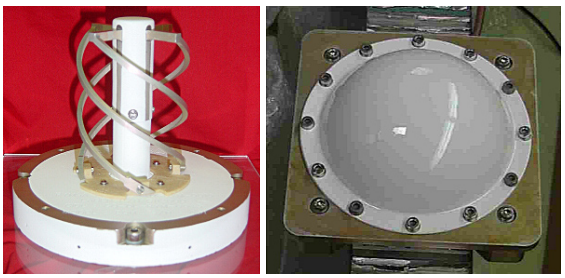

Fig. 7: Engineering models of Quadrifilar Helix Antenna from RYMSA (left) and DM-C146 Patch Antenna (right)

antennas which implies that they do not have any integrated low noise preamplifier. Hence, the two on-board LAGRANGE GPS receivers are completely responsible for an adequate signal amplification.

The Quadrifilar Helix antenna was developed specifically for the GOCE SSTI application by RYMSA, Spain. The positions of the antenna with respect to the solar wing have been optimized by electromagnetic simulations in order to minimize any interactions with the spacecraft. To ensure that the signal level is sufficient to receive satellite signals from all direction, the antenna provides a broad gain pattern with a very sharp drop-off near the horizon in order to minimize multipath interferences coming from the spacecraft body. Moreover, the antenna was designed with high rejection to Left Hand Circularly Polarized (LHCP) signals. Hence, multipath effects will be further reduced because the direct GPS satellite signal is Right Hand Circularly Polarized (RHCP) whereas received multipath signals caused by one or an odd number of reflections are LHCP. Due to the unsymmetrical structure of the antenna feeding part and the fact that the number of turns of the helical arms is equal to 2/3, significant azimuthal phase variations can be expected.

In terms of risk mitigation, a second antenna model called DM-C146 was selected in order to have a possible back-up solution. Moreover, tests on this antenna were executed in order to have a reference for assessing the performance of the Quadrifilar Helix antenna. The DM-C146 contains a standard Dorne Margolin C-146-10 patch element. It is covered by a plastic housing and has a metallic ground plane in a square shape. Therefore, also significant azimuthal phase variations can be expected. Other than the Quadrifilar Helix, the position of the antenna with respect to the solar wing has not been optimized. Hence, one can expect that the near field influence on the DM-C146 Patch antenna will be conspicuously stronger.

4 GOCE SSTI Antenna Calibration

The GOCE SSTI antenna calibration campaign was executed in April 2005 on the rooftop of the Institut für Erdmessung. Several experiments were performed in order to characterize phase center offsets, phase variations and carrier to noise behaviour of the two antenna test candidates. All GPS measurement data have been modelled via spherical harmonic expansions of degree 8 and order 5, which has been adopted and verified from the calibration of regular antenna types. Each antenna was calibrated once mounted in stand-alone mode and once mounted on a simplified GOCE spacecraft model. The differences between both set-ups in terms of the phase variation characteristics and the carrier to noise ratio show the near field influence of the satellite model on the particular test antenna.

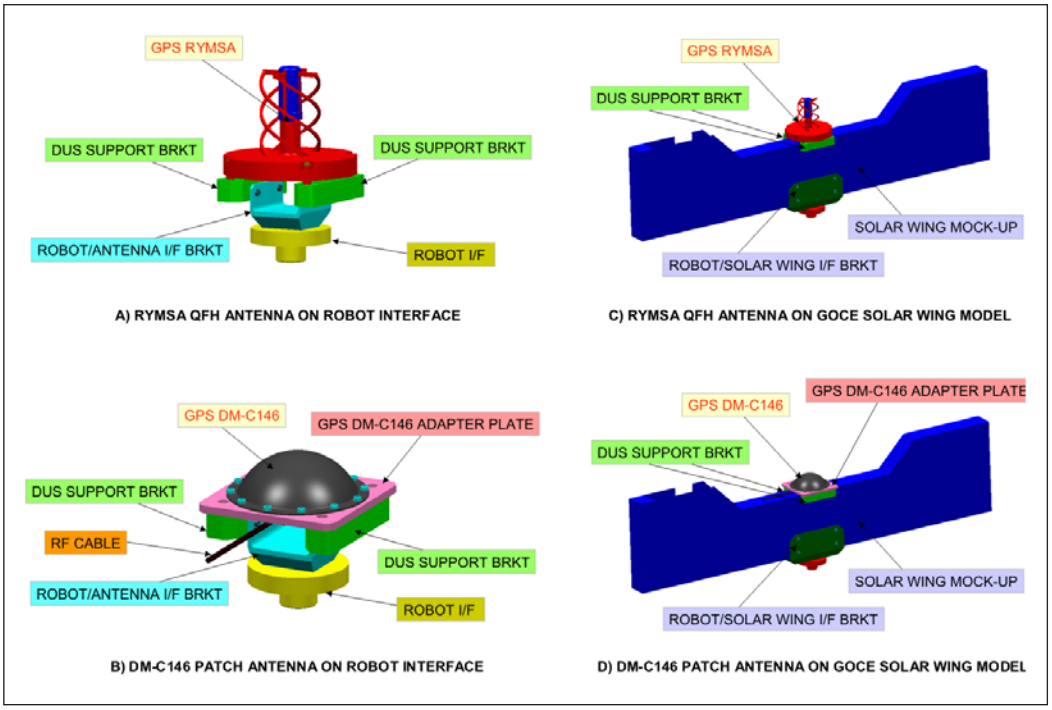

Fig. 8: Mechanical set-ups for robot calibration campaign (provided by ESA/AAS-I)

Unfortunately, the original GPS receiver of the SSTI instrument was not available for the Hannover test campaign. Instead, a Javad Legacy RX has been used by placing an external inline amplifier after the antenna output to provide a gain of 20 dB. An antenna cable length of approximately 2 m was chosen in order to minimize further signal loss. In addition, it was necessary to block the amplifier DC voltage in order to avoid short-circuit. For this purpose, a DC decoupler was connected between amplifier and antenna. The PCV signal as well as the decrease of the C/No are not affected by the presence of the inline amplifier and the DC decoupler.

Concerning size and weight, the robot has a limited capability to handle antenna constructions. Therefore, only a small model of the GOCE spacecraft could be used for the simulation of the antenna environment (Fig. 3). The results consequently refer to the simplified model and do not show the overall influence of the spacecraft. The model is taken as a cut-out of the original spacecraft's solar wing and has a dimension of $1300 \times 65 \times 300\,\mathrm{mm}^3$. The side walls consist of a carbon-fiber skin with an internal structure of aluminium. The top surface is characterized by a metallic honeycomb structure with cells having a size of about 1 cm. In addition to the calibrations using the non-uniform honeycomb structure, the wing was covered by a flat metallic tape in order to evaluate and compare the influence of these two different types of surfaces.

The GOCE solar wing model was mounted beneath the particular antenna test candidate in that way that the direction of its longitudinal axis corresponds exactly to an azimuth of 0° respectively 180° within the antenna reference system. One can expect that the most significant near field effects will affect these regions of the PCV and C/No pattern. In order to be able to connect the antenna to the robot arm and to the solar wing model, several metallic interface brackets were mounted beneath the antenna and the wing. The assembled mechanical set-ups are shown in Fig. 8.

5 Results

5.1 Antenna Calibrations with Solar Wing

The phase variations of both antenna types mounted on the GOCE solar wing model are illustrated in Fig. 10 and Fig. 11. The patterns refer to the particular mean phase center offset and show variations in azimuth and elevation of up to ±16 mm in case of the Quadrifilar Helix and ±30 mm in case of the DM-C146 Patch configuration. Remembering the GOCE SSTI requirements on the phase center knowledge, the determined variations definitely have to be considered in the orbit data processing. One single set of mean phase center offsets is not sufficient to characterize the entire antennas with the required accuracy.

5.2 Solar Wing vs. Stand-alone Set-up

5.2.1 Differences of Phase Center Offsets

In order to give a first impression on how the phase variation behaviour of the isolated antenna has changed in average due to the presence of the GOCE solar wing model, differences of the particular phase center offset components were computed (Fig. 9). One can observe that the mean phase center has obviously shifted within several millimeters. Here, it is interesting to notice that the presence of the wing mainly modifies the x- and z-components whereas changes in the y-coordinate of the offset (i. e. across the wing) are far below 1 mm. This is valid for each test configuration and carrier signal. As expected, the DM-C146 antenna is more affected by the solar wing, which might be to some extend to its non-optimized position. For a more detailed analysis, one has to turn attention to the differences of the individual phase variations.

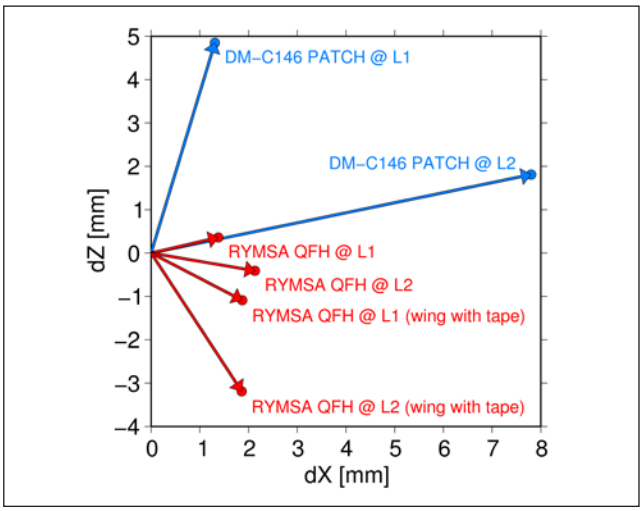

Fig. 9: Shifting of the mean phase center offset components x and z due to the presence of the GOCE solar wing model

5.2.2 Differences of Phase Variations

In order to accomplish a rigorous comparison between different calibration results, phase variations must always refer to one identical reference point. Therefore, all PCV data sets are converted to the antenna reference point at the bottom of the particular test antenna housing and finally differences between data grids of 5° have been computed. The results showing the differences between stand-alone and solar wing calibration for each antenna model and the particular frequency are presented in Fig. 12 and Fig. 13. Numerical statistics according to different elevation cut-off angles are summarized in Table 1 and Table 2.

The outcome of the analysis is that the presence of the solar wing model introduces significant ripples in the PCV pattern of up to ±1 cm in case of the Quadrifilar Helix and even up to ±3 cm in case of the DM-C146 Patch configuration. In this context, it has been verified that using a flat surface for the wing instead of a honeycomb structure does not induce considerable changes. The reason for this can be found in the honeycomb cell size of just 1 cm which is quite small with respect to the GPS carrier phase wavelengths. As already indicated from the offset comparison, the maximum ripples for the original GPS carrier signals appear near the horizon under an azimuth of 0° respectively 180°. This direction corresponds exactly to the alignment of the wing. Furthermore, it can be noticed that the near field effects on the L2 signal are always stronger than on L1. This can be caused partly by the longer carrier wavelength of L2, which can principally give a higher maximum multipath error (Georgiadou and Kleusberg 1988). Forming the ionospheric-free linear combination L0, the effect on RMS is amplified once more by a factor of about 2 to 3 and consequently modifies the phase variations of the entire antenna hemisphere.

The magnitude as well as the fact that the measured solar wing effects on the phase variations are more evident around the antenna horizon has been confirmed independently at ESA/ESTEC by extensive electromagnetic simulations using the commercial software package FEKO. The program requires that the entire antenna structure is broken down into several ten-thousand wire segments

Tab. 1: Near field influences of GOCE solar wing model on phase variations of RYMSA QFH antenna

Carrier Signal	Elevation Cut-Off	MIN [mm]	MAX [mm]	RMS [mm]
L0	0°	−11.3	+10.5	±4.1
	15°	−6.8	+10.5	±3.7
L1	0°	−4.8	+9.0	±1.8
	15°	−3.8	+5.6	±1.4
L2	0°	−4.7	+11.4	±1.9
	15°	−4.7	+4.7	±1.5

Tab. 2: Near field influences of GOCE solar wing model on phase variations of DM-C146 Patch antenna

Carrier Signal	Elevation Cut-Off	MIN [mm]	MAX [mm]	RMS [mm]
L0	0°	−30.2	+30.6	±12.4
	15°	−20.0	+30.6	±11.7
L1	0°	−8.6	+20.9	±4.1
	15°	−3.7	+8.0	±3.0
L2	0°	−16.7	+31.2	±7.7
	15°	−13.9	+24.1	±6.3

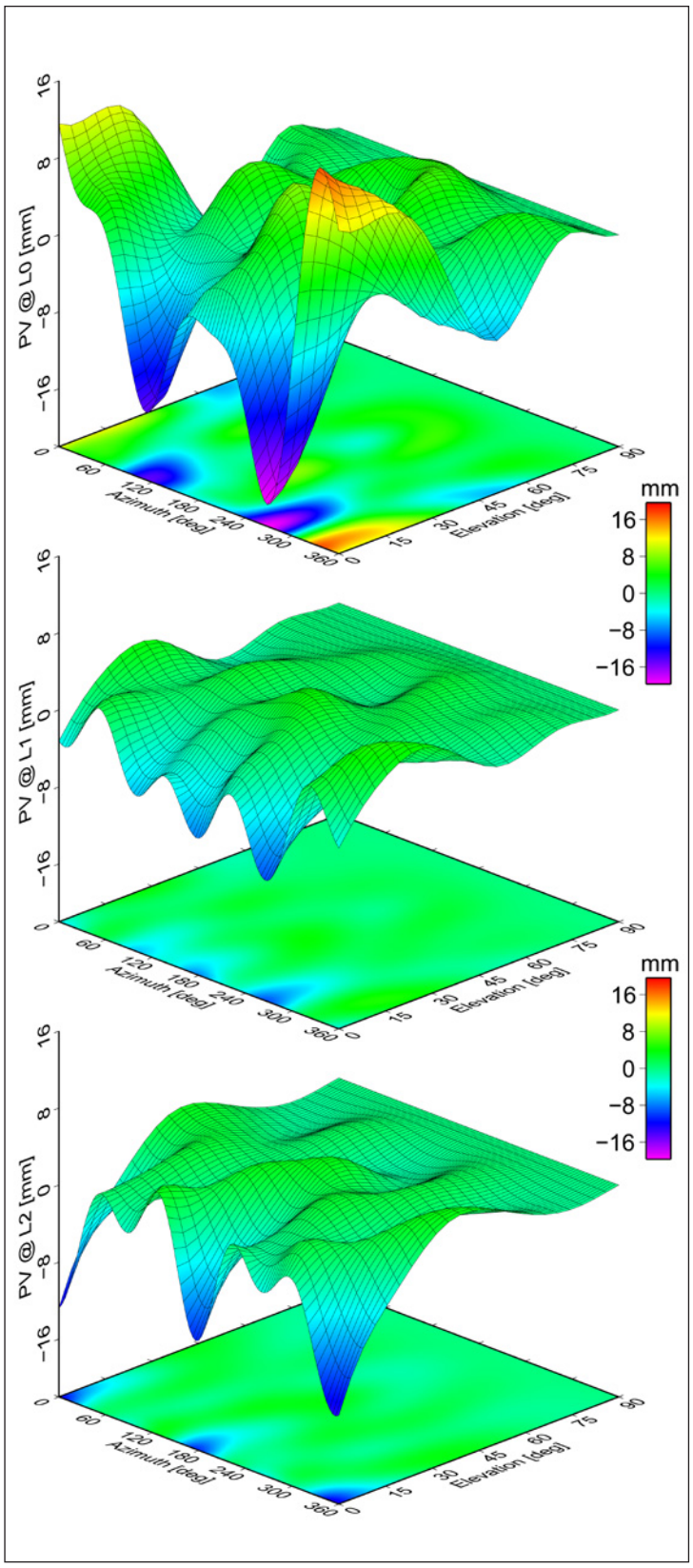

Fig. 10: Phase variations with respect to mean phase center offset of RYMSA Quadrifilar Helix antenna mounted on GOCE solar wing model

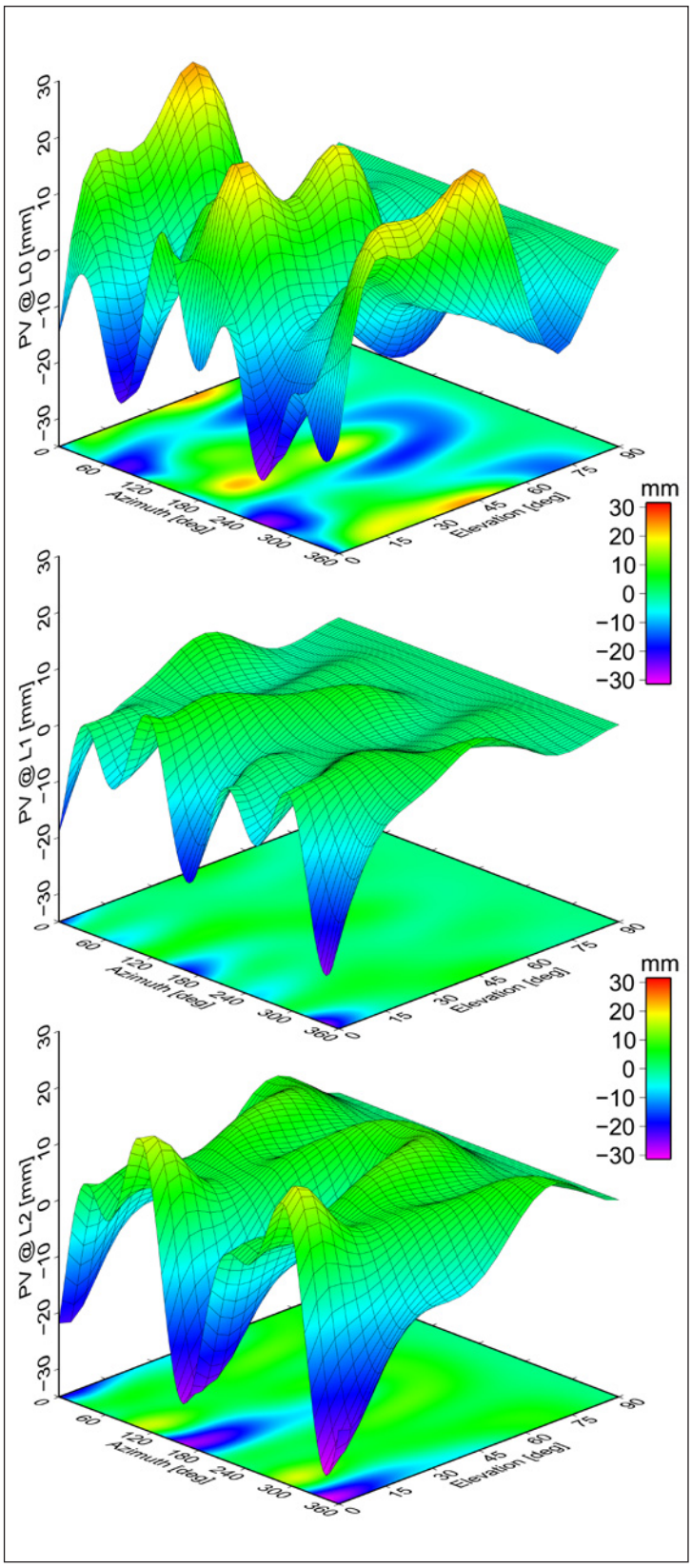

Fig. 11: Phase variations with respect to mean phase center offset of DM-C146 Patch antenna mounted on GOCE solar wing model

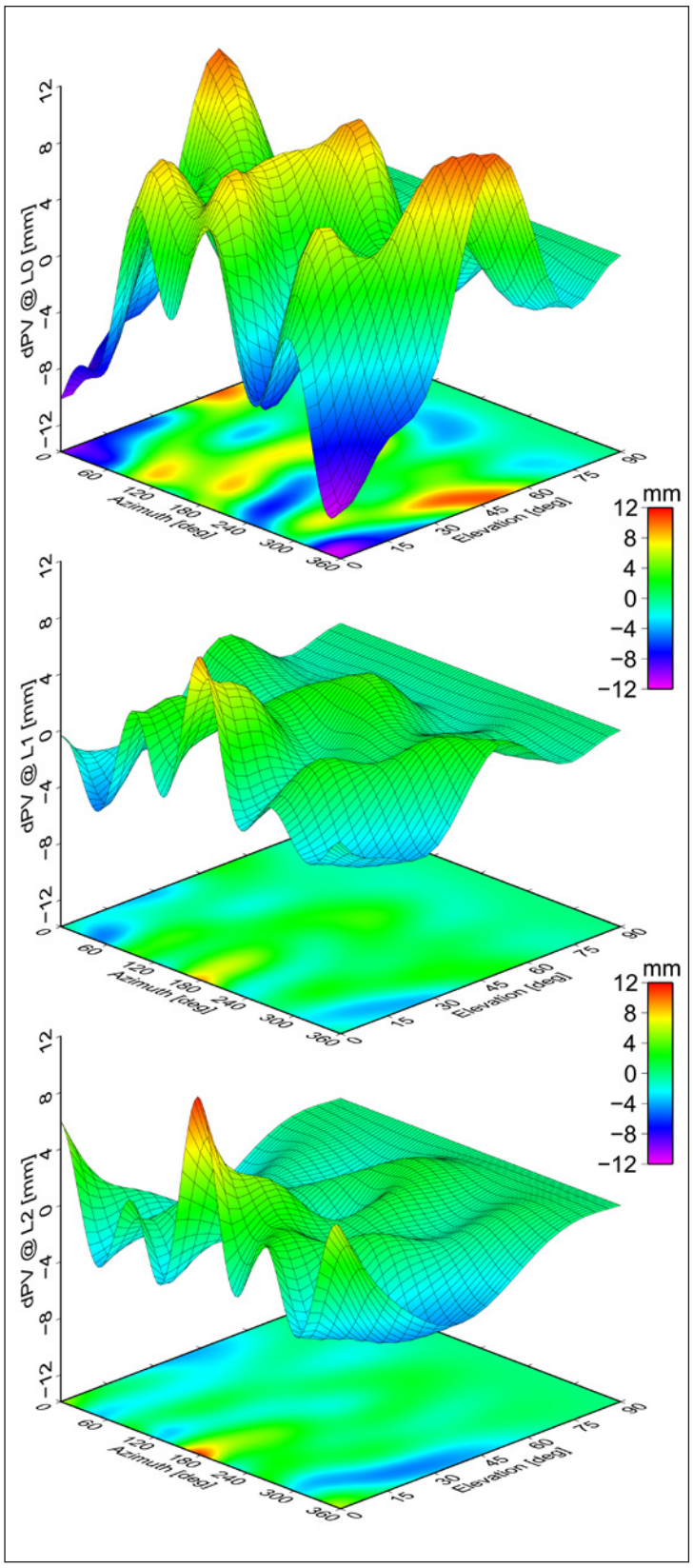

Fig. 12: Near field influences of GOCE solar wing model on phase variations of RYMSA Quadrifilar Helix antenna

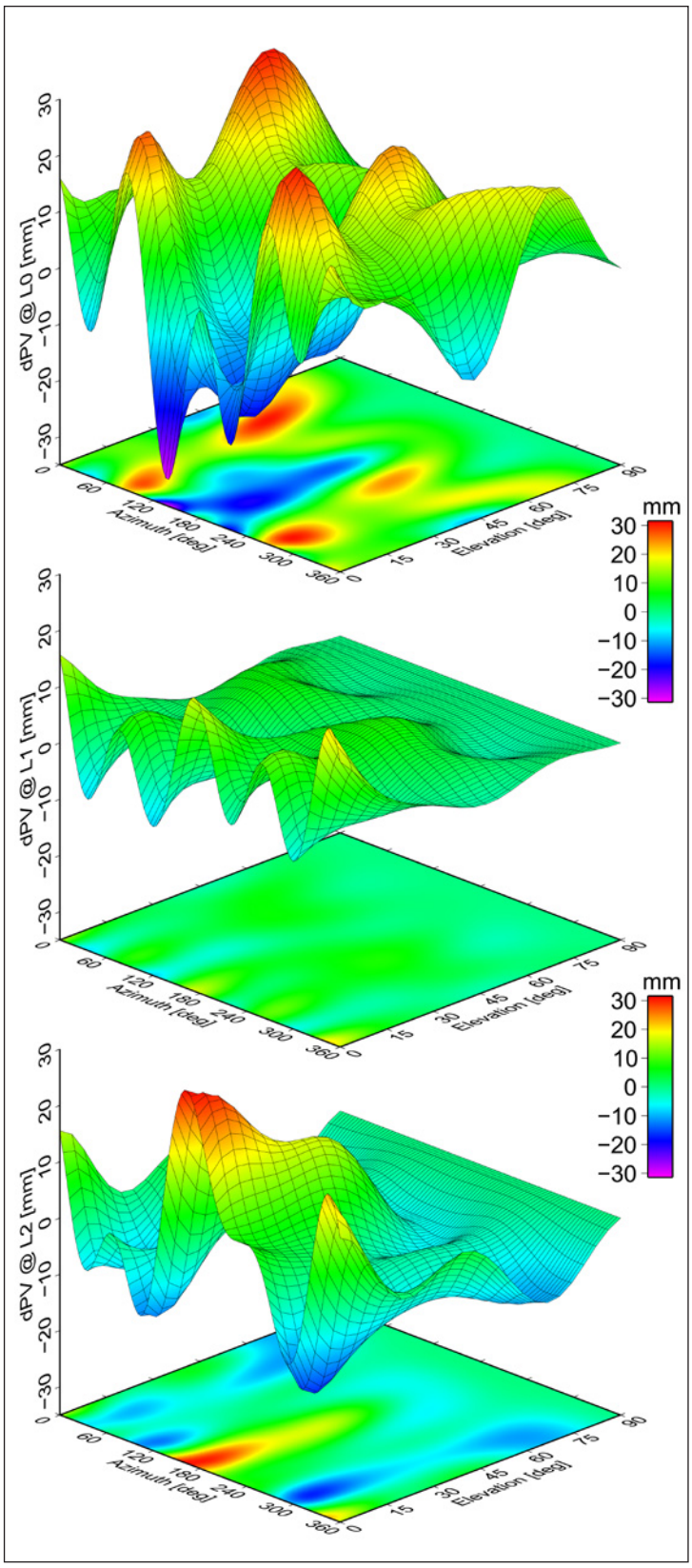

Fig. 13: Near field influences of GOCE solar wing model on phase variations of DM-C146 Patch antenna

and surface patches. Once a model is defined, the so-called Method of Moments (MoM) technique is used to solve for the unknown wire and surface currents. If the current distribution is known, further parameters like the near field, far field, directivity or input impedance of an antenna may be obtained. By this means, phase and gain pattern of the Quadrifilar Helix antenna were simulated for the isolated antenna and for the case it is installed on diverse GOCE satellite models. Results are given in Polimeni (2004) and Toso et al. (2005). Further investigations are currently underway.

5.2.3 Differences of Carrier to Noise

The pattern of the carrier to noise decrease depends on the actual antenna/receiver pair. Therefore, the C/No results of the present calibration campaign can only give some indications of the antenna gain behaviour.

The comparison of the C/No characteristics between stand-alone and solar wing calibration point out no significant differences in case of the Quadrifilar Helix configuration. Covering the wing model with a flat surface instead of using the rough honeycomb structure does also not cause significant changes of C/No. The signals were logged by the receiver with a resolution of 1 dB-Hz. With respect to this value, deviations of just 1 to 2 dB-Hz lead to the conclusion that the presence of the wing does not introduce any important degradation on the GOCE SSTI performance in terms of the antenna gain pattern. The electromagnetic computations of the antenna gain pattern done at ESA/ESTEC confirm these results even for the case of simulating the environment of the entire spacecraft.

However, the calibrations of the DM-C146 Patch antenna show that the solar wing model induces clear asymmetries of about 3 dB-Hz on L1 and amplifies and/or attenuates the signal strength on L2 constantly around 5 dB-Hz. Following the well known rule of thumb that 3 dB-Hz is equal to half or double the signal power level, one can notice that possibly the influence of the wing on the antenna gain can be quite strong. Referring to this issue, more results are given in Dilßner and Seeber (2005).

5.2.4 Effects on Precise Orbit Determination

Depending on the particular GPS satellite constellation, neglecting the above described antenna near field influence on the PCV pattern will seriously affect the final point positioning solution of the GOCE SSTI application. Orbit investigations done at IfE based on GOCE and GPS simulation data of the University of Bonn show a position dilution of precision (PDOP) of 1 to 3 using all available GPS satellites above the horizon of the GOCE spacecraft and a value of 2 to 10 using an elevation mask of 15°. Under these conditions, the resulting decrease in positioning accuracy σ_p can be estimated in rough approximation using the well known relationsship

$$\sigma_p = \sigma_r \cdot PDOP \tag{3}$$

between measurement and position domain (Seeber 2003). Consequently, a mean phase error σ_r of about ±4 mm in case of the ionospheric-free signal of the Quadrifilar Helix antenna configuration would give rise to positioning uncertainties of around ±4 to 12 mm using a 0° cut-off angle and even of around ±8 to 40 mm using 15°. Of course, the estimation is not rigorous and rather pessimistic, because the systematic character of the phase variations is neglected and correlations with respect to additional unknown parameters (e. g. GPS satellite orbits and clocks) are not taken into account.

For a more reliable estimation of the antenna near field effect on the positional accuracy of the GOCE spacecraft, we refer to a kinematic POD study performed at the Technical University of Munich using a joint orbit simulation of GOCE and GPS satellites (Svehla and Rothacher 2005). The data processing has been done with the Bernese v5.0 software package using a kinematic approach based on zero-differenced ionospheric-free carrier phase observations. Positions have been computed over a period of 24 hours. Two different simulations based on phase corrections from our calibration tests, once obtained by the robot stand-alone calibration and once using the corrections obtained with the solar wing configuration, were conducted. The coordinate differences of both computations based on the corrections of the Quadrifilar Helix antenna are illustrated in Svehla and Rothacher 2005. Neglecting the near field influences in the simulations leads to an additional 3D-RMS error in the precise orbit determination of 35 mm for the use of all satellites above the antenna horizon and even up to 51 mm using an elevation cut-off angle of 15°. These results confirm the need for adequate antenna correction in the POD data processing.

6 Summary and Conclusions

As anticipated by GOCE project, the SSTI antenna calibration results are essential for achieving the required accuracy level in precise orbit determination for the ESA GOCE mission to be launched in 2007. The magnitude of the determined antenna phase center offsets and variations show and confirm the need to take PCV corrections into account to fully meet the accuracy requirements when processing the orbit positions of the GOCE spacecraft. Additionally, near field effects like multipath disturbances have to be considered as they can conspicuously modify the measurement performance. Depending on carrier frequency, antenna type and position, one can ob-

serve that the presence of the spacecraft's solar wing can cause changes of up to 3 cm in phase and 5 dB-Hz in amplitude. Because the wing had been specifically designed for accommodating the Quadrifilar Helix antenna, near field effects are considerably smaller compared to the DM-C146 antenna configuration. The results of the Helix antenna have been obtained on a RYMSA engineering model whereas preliminary first measurements on the final flight-models already indicate further performance improvement.

In case of the GOCE mission, special attention needs to be paid to the ionospheric-free signal L0 which amplifies antenna phase variations and near field effects once more by a factor of 3. This linear combination is of particular relevance for the satellite, because for a mean orbital altitude of 250 km ionospheric propagation delays still play a non-negligible role. Kinematic POD simulations based on ionospheric-free observations demonstrate that the impact of the near field effects on the positioning accuracy of the GOCE spacecraft can be about 5 cm in 3D-RMS. The Automated Absolute Field Calibration developed by IfE and Geo++ has proven to be one powerful means to determine suitable corrections for antenna phase variations and near field effects.

Acknowledgements

The work described in this article was funded by the European Space Agency (ESA). The preparation and execution of the robot calibration campaign was supported by Alcatel Alenia Space Italy (AAS-I) from Turin.

References

Dilßner, F., Seeber, G.: Absolute Field Calibration of the GOCE GPS Antennas RYMSA Quadrifilar Helix and LABEN Cosmo Patch. Test Report for the European Space Research and Technology Centre (ESTEC), Hannover, 2005.

Elosegui, P., Davis, J.L., Jaldehag, R.K., Johansson, J.M., Niell, A.E., Shapiro, I.I.: Geodesy using the Global Positioning System: The effects of signal scattering on estimates of site position. Journal of Geophysical Research-Solid Earth, 100, pp. 9921–9934, 1995.

Georgiadou, Y., Kleusberg, A.: On carrier signal multipath effects in relative GPS positioning. Manuscripta geodaetica, Vol. 13, pp. 172–179, 1988.

Gendt, G., Schmid, R.: Planned changes to IGS antenna calibrations. IGS Electronic Mail, Message Number 5189, 2005.

Gendt, G.: Switch the absolute antenna model within the IGS. IGS Electronic Mail, Message Number 5272, 2005.

Görres, B., Campbell, J., Siemes, M., Becker, M.: New anechoic chamber results and comparison with field and robot techniques. Presented at the IGS Workshop 2004, Bern, Switzerland, 2004.

Langley, R.B.: GPS Receiver System Noise. GPS-World, June 1997, pp. 40–45, 1997.

Mader, G.L.: GPS Antenna Calibration at the National Geodetic Survey. GPS Solutions, 3(1), pp. 50–58, 1999.

Menge, F.: Zur Kalibrierung der Phasenzentrumsvariationen von GPS-Antennen für die hochpräzise Positionsbestimmung. Wissenschaftliche Arbeiten der Fachrichtung Vermessungswesen an der Universität Hannover, Nr. 247, 2003.

Polimeni, D.: GOCE SSTI Antenna Performance. ESTEC Working Paper No. GO-RP-ESA-0119-2004, Noordwijk, 2004.

Schmitz, M., Wübbena, G., Boettcher, G.: Near Field Effects of a Car Roof on TPSHIPERPLUS Phase Variations. Http://www.geopp.com/publications, Garbsen, 2004.

Schupler, B.R., Allshouse, R.L., Clark, T.A.: Signal Characteristics of GPS User Antennas. J. Inst. Navigation, 41, pp. 277–295, 1994.

Seeber, G.: Satellite Geodesy. 2nd Edition. W. de Gruyter, Berlin, New York, 2003.

Svehla, D., Rothacher, M.: First LEO Satellite Constellation Based on GPS. Presented at the AGU Fall Meeting 2005, San Francisco, 2005.

Toso, G., Maeusli, D., Polimeni, D., Nepa, P.: Analysis of GOCE SSTI/GPS Antenna Performance. Presented at the 28th ESA Antenna Workshop 2005, Noordwijk, 2005.

Weill, L.R.: Multipath Mitigation: How Good Can It Get with New Signals? GPS-World, June 2003, pp. 106–113, 2003.

Wübbena, G., Schmitz, M., Menge, F., Böder, V., Seeber, G.: Automated Absolute Field Calibration of GPS Antennas in Real-Time. Proceed. ION GPS-2000, pp. 2514–2522, 2000.

Wübbena, G., Schmitz, M., Boettcher, G.: Zum Einfluss des Antennennahfeldes. Presented at the 5th GPS Antenna Workshop 2003, Frankfurt/Main, 2003.

Authors' address

Florian Dilßner | Günter Seeber
Institut für Erdmessung
Universität Hannover
Schneiderberg 50, 30167 Hannover, Germany
dilssner@ife.uni-hannover.de | seeber@ife.uni-hannover.de

Martin Schmitz | Gerhard Wübbena
Geo++ GmbH
Steinriede 8, 30827 Garbsen, Germany
martin.schmitz@geopp.de | gerhard.wuebbena@geopp.de

Giovanni Toso | Damien Maeusli
European Space Research and Technology Centre (ESTEC)
Kepleraan 1, P.O. Box 299, 2200 AG Noordwijk ZH, Netherlands
giovanni.toso@esa.int | damien.maeusli@esa.int